J|A|C|S
ARTICLES
Published on Web 02/10/2006

A Combined Kinetic−Quantum Mechanical Model for Assessment of Catalytic Cycles: Application to Cross-Coupling and Heck Reactions

Sebastian Kozuch and Sason Shaik*

Contribution from the Department of Organic Chemistry and The Lise Meitner-Minerva Center for Computational Quantum Chemistry, Givat Ram Campus, Jerusalem 91904, Israel

Received August 27, 2005; E-mail: sason@yfaat.ch.huji.ac.il

Abstract: The efficiency of catalytic cycles is measured by their turnover frequency (TOF). The degree of TOF control determines which states contribute most to the rate of the cycle, and thus indicates the steps that have the highest impact on the cycle. A kinetic model developed by Christiansen (Christiansen, J. A. *Adv. Catal.* **1953**, *5*, 311) for catalytic cycles is implemented here in a form that utilizes state energies. This enables one to assess the efficiency of quantum mechanically computed catalytic cycles like the palladium-catalyzed cross-coupling and Heck reactions, to test alternative hypotheses, and to make some predictions. This implementation can also account for effects such as Sabatier's volcano curve for heterogeneous catalysis. The model leads to a dependence of the TOF for any cycle on the "corrected" energy span quantity, δE, whose precise expression depends on the location of the summit and trough of the cycle in the step sequence of the cycle. Thus, knowing the highest energy transition state, the most abundant reaction intermediate, and the reaction energy enables one to make quick predictions about relative efficiency of cycles. At the same time, the degree of TOF control determines which states contribute most to the rate of reaction, and thus indicates the values to be included in the calculation of the energetic span and the steps that may be tinkered with to improve the cycle.

Introduction

Catalytic cycles (Scheme 1) are ubiquitous in chemistry and biology; most enzymes operate by means of catalytic cycles, and efficient catalysts are those that lead to a large turnover frequency (TOF) of the cycle. How one can conceptualize an efficient catalytic cycle is the main concern of the present contribution that seeks to combine the insights of quantum chemistry with a kinetic model that permits a detailed calculation of relative efficiencies.

Modern quantum mechanical (QM) modeling of catalysts provides us with detailed insight into the energy landscape of a given catalytic cycle. The quantitative aspects of these studies have been greatly improved in recent years, mostly due to the advent of density functional theory (DFT) that allows generally reliable computations to be made for catalytic processes.[1−3] Even enzymatic cycles for species with thousands of atoms can be calculated today by use of the hybrid DFT/molecular mechanics (DFT/MM) method.[4] A useful addition to these sophisticated treatments would be an integrating tool that can answer the key question: *How efficient is a given catalytic cycle vis-à-vis an alternative one?* Many QM treatments, as well as experimental assessments of catalysts, tend to focus on the rate-determining step of the cycle, i.e., the one possessing the highest transition state (HETS), and try to find a catalyst that lowers the energy of that specific transition state. However, this approach, while very good for revealing trends under single turnover conditions, misses an essential property of a catalyst, the TOF of its catalytic cycle. The TOF of a cycle does not depend on the rate-determining step or any other single factor; it is rather an

Scheme 1. A Schematic Catalytic Cycle with an Energy Difference of ΔG (the Reaction Energy of One Turnover)[a]

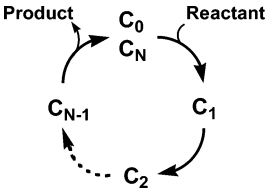

[a] The starting and final stages of the catalyst species (C_0 and C_N) are essentially the same molecular state.

(1) For a tiny selection of papers focused on the perspectives of quantum studies of catalysis, see: (a) Frenking G.; Fröhlich N. *Chem. Rev.* **2000**, *100*, 717−774. (b) Cundari, T. R.; Deng, J.; Fu, W.; Klinckman, T. R.; Yoshikawa, A. *J. Chem. Inf. Comput. Sci.* **1998**, *38*, 941−948. (c) Neurock, M. *J. Catal.* **2003**, *216*, 73−88. (d) Gokhale, A. A.; Kandoi, S.; Greeley, J. P.; Mavrikakis, M.; Dumesic, J. A. *Chem. Eng. Sci.* **2004**, *59*, 4679−4691. (e) Boudart, M. *Catal. Lett.* **2000**, *65*, 1−3. (f) Greeley, J.; Mavrikakis, M. *Nat. Mater*. **2004**, *3*, 810−815. (g) Sundermann, A.; Uzan, O.; Martin J. M. L. *Chem. Eur. J.* **2001**, *7*, 1703−1711 (h) Braga, A.; Morgon, N.; Ujaque, G.; Maseras, F. *J. Am. Chem. Soc.* **2005**, *127*, 9298−9307. (i) Senn, H. M.; Ziegler, T. *Organometallics* **2004**, *23*, 2980. (j) Jacoby, M. *Chem. Eng. News* **2004**, *82* (Nov 29), 25−28.

(2) Kozuch, S.; Jutand, A.; Amatore, C.; Shaik, S. *Organometallics* **2005**, *24*, 2319−2330.

(3) Goossen, L. J.; Koley, D.; Hermann, H. L.; Thiel, W. *J. Am. Chem. Soc*. **2005**, *127*, 11102−11114.

(4) See, for example, the computed catalytic cycle of cytochrome P450: (a) Loew, G. H.; Harris, D. L. *Chem. Rev*. **2000**, *100*, 407−420. (b) Shaik, S.; Kumar, D.; de Visser, S. P.; Altun, A.; Thiel, W. *Chem. Rev.* **2005**, *105*, 2279−2328.

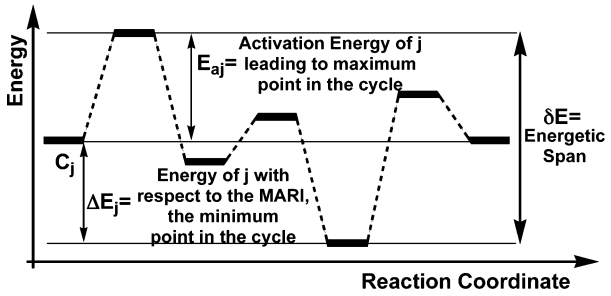

Figure 1. Schematic representation of a catalytic cycle. A simplified analysis shows that the factor that determines the efficiency of the cycle is the energy span, δE, rather than the activation energy, Ea_j, of the rate-determining step.

integrated "rate function" of the entire cycle, the nano-machine that carries the catalysis.

In this contribution, we develop a kinetic model that uses computational QM data and enables one to answer key questions associated with a catalytic cycle, such as the one presented in Scheme 1. The kinetic model is based on the steady-state approximation.[5] For convenience, the expressions are based on fixed standard concentrations of the noncatalyst species (reactant, product, and cofactors), but this convenience can be waived and the treatment can be modified to consider variable concentrations. The so-developed model is designed to attend QM calculations to predict the TOF and its variation using the normally calculated quantities, barriers, and relative energies of intermediates, reactants, and products. The model is subsequently applied here to the various versions of the catalytic cycle for the palladium-catalyzed cross-coupling and Heck reactions studied previously by a few groups,[2,3,6] as well as to Sabatier's volcano effect in heterogeneous catalysis[7,8] and its connection to the Brønsted coefficients and the Bell−Evans−Polanyi principle.[9]

What Makes for a Good Catalytic Cycle? A brief background that provides insight into the question has been given by Amatore and Jutand.[10] Consider, in Figure 1, the velocity of a catalytic process when steady-state kinetics is reached. In this case, one can use the Eyring equation or the Arrhenius rate law and express the rate (r) of the cycle approximately as in eq 1:

$$r \approx [C_j]k_j = [C_j]A\, e^{-Ea_j/RT} \qquad (1)$$

where C_j is the catalyst species of the rate-determining step and Ea_j is the corresponding activation energy. A rough estimate of the concentration of C_j can be achieved considering the respective Boltzmann distribution,

$$[C_j] \approx [C_t]\, e^{-\Delta E_j/RT} \qquad (2)$$

where $[C_t]$ is the total concentration of catalyst species and ΔE_j is the energy of C_j with respect to the lowest-lying intermediate, also known as the most abundant reaction intermediate (MARI).[11,12] This leads to the following expressions for the rate, r, and TOF of the cycle:

$$\mathrm{TOF} = \frac{r}{[C_t]} \approx A\, e^{-(Ea_j + \Delta E_j)/RT} = A\, e^{-\delta E/RT} \qquad (3)$$

Here δE is called the energetic span of the cycle,[10] which by reference to Figure 1 is the difference between the highest and the lowest points (the highest is the HETS and the lowest is the MARI) of the catalytic cycle. Thus, according to this approximate treatment, the energetic span factor determines the frequency of the catalytic cycle, namely *the turnover frequency*, TOF (cycles per time and catalyst concentration), of the cycle. Thus, even a simplified treatment shows that the efficiency of the cycle is determined by more than just the rate-determining step, and generally, an efficient cycle requires a relatively flat energy landscape.

As shall be seen later, there are other essential requirements for a large TOF. Thus, the δE quantity is a suitable measure of TOF only when the energetic span is much larger than the reaction energy of the cycle, ΔG (the energy difference between the starting and ending points of one turnover). But whereas ΔG is independent of the catalyst, the energies of the intermediates and transition states are all catalyst-dependent, and this is the key for any kinetic influence of all these species on the more precise expression of the TOF of the cycle, as presented in this paper, which connects the TOF to the energy landscape computed by QM methods.

Theoretical and Computational Methods

The kinetic features of a simple cyclic reaction at steady state can be calculated following the treatments of Christiansen[5,13] and Campbell[14,15] with some modifications associated with the goal to link the kinetic model to QM results. Christiansen provided an exact method to calculate the TOF of an N-step catalytic cycle as in Scheme 1, while Campbell's degree of rate control allows us to probe the effect of any step on the kinetics of the cycle.

Calculation of the TOF. For a catalytic cycle (Scheme 1) at a steady-state regime,[5,13,16] all the changes in the concentration with time are zero, and therefore, the rates of all the processes must be the same and equal to the global rate r in eq 4:

$$r = k_1C_0 - k_{-1}C_1 = k_2C_1 - k_{-2}C_2 = ... = k_NC_{N-1} - k_{-N}C_N \qquad (4)$$

This set of linear equations can be written in a matrix form, which for a cycle with four species is the following:

$$\begin{pmatrix} r_1 & -r_{-1} & 0 & 0 \\ 0 & r_2 & -r_{-2} & 0 \\ 0 & 0 & r_3 & -r_{-3} \\ -r_{-4} & 0 & 0 & r_4 \end{pmatrix} \begin{pmatrix} [C_1] \\ [C_2] \\ [C_3] \\ [C_4] \end{pmatrix} = \begin{pmatrix} 1 \\ 1 \\ 1 \\ 1 \end{pmatrix} \qquad (5)$$

Here, r_i is an individual rate constant scaled by the global rate, i.e., $r_i = k_i/r$. As shown by Christiansen,[5,13] the TOF (number of cycles per

(5) Boudart, M. *Kinetics of Chemical Processes*; Prentice-Hall Inc.: Englewood Cliffs, NJ, 1968; pp 67−71.
(6) Lin, B.; Liu, L.; Fu, Y.; Luo, Sh.; Chen, Q.; Guo, Q. *Organometallics* **2004**, *23*, 2114−2123.
(7) Bligaard, T.; Nørskov, J. K.; Dahl, S.; Matthiesen, J.; Christensen, C. H.; Sehested, J. *J. Catal.* **2004**, *224*, 206−217.
(8) Jacobsen, C.; Dahl, S.; Clausen, B. S.; Bahn, S.; Logadottir, A.; Nørskov, J. K. *J. Am. Chem. Soc.* **2001**, *123*, 8404−8405.
(9) Mayer, J. M. *Acc. Chem. Res.* **1998**, *31*, 441.
(10) Amatore, C.; Jutand, A. *J. Organomet. Chem.* **1999**, *576*, 254−278.
(11) Stolze, P. *Prog. Surf. Sci.* **2000**, *65*, 65−150.
(12) Boudart, M.; Djéga-Mariadassou, G. *J. Catal.* **2003**, *216*, 89−97.
(13) Christiansen, J. A. *Adv. Catal.* **1953**, *5*, 311.
(14) Campbell, C. T. *Top. Catal.* **1994**, *1*, 353.
(15) Campbell, C. T. *J. Catal.* **2001**, *204*, 520−524.
(16) Experimentally, the induction time to reach a steady state may vary substantially for each reaction. In the case of Pd cycles, it can be on the order of an hour at 60 °C after ~25 turnovers. This is dependent, e.g., on the time required to reach the right catalyst starting point from the precatalysts, plus the time required for stabilization of the concentration of all the catalyst species. Kinetic measurements will result in erroneous deduction of rate expressions and mechanisms if the induction time is not reached (Buchwald, S. L. *J. Am. Chem. Soc.* **2002**, *124*, 14104−14114).

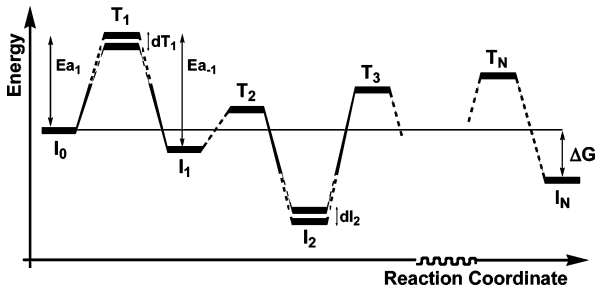

Figure 2. A single turnover in a catalytic cycle, with indications of the various energy quantities, and the energy changes of two species that affect the degree of TOF control.

time unit and catalyst concentration) can be expressed as in eq 6a:

$$\mathrm{TOF} = \frac{\Delta}{M} \tag{6a}$$

where Δ is the difference between the products of the forward rate constants and the reverse ones, defined in eq 6b.

$$\Delta = k_1 k_2 \ldots k_N - k_{-1} k_{-2} \ldots k_{-N} \tag{6b}$$

The quantity M is the sum of all the elements of the matrix $\hat{M}$, eqs 6c and 6d; the first element is the product of rate constants from k_2 to k_N and others are generated by the permutations of one of the k_i's per matrix element:

$$M = \sum_{a,b} M_{a,b} \tag{6c}$$

$$\hat{M} = \begin{pmatrix} k_2k_3k_4\ldots k_N & k_{-1}k_3k_4\ldots k_N & k_{-1}k_{-2}k_4\ldots k_N & \cdots & k_{-1}k_{-2}k_{-3}\ldots k_{-(N-1)} \\ k_3k_4\ldots k_Nk_1 & k_{-2}k_4\ldots k_Nk_1 & k_{-2}k_{-3}\ldots k_Nk_1 & \cdots & k_{-2}k_{-3}\ldots k_{-(N-1)}k_{-N} \\ \vdots & \vdots & \vdots & \ddots & \vdots \\ k_Nk_1k_2\ldots k_{N-2} & k_{-(N-1)}k_1k_2\ldots k_{N-2} & k_{-(N-1)}k_{-N}k_2\ldots k_{N-2} & \cdots & k_{-N}k_{-(N-1)}k_{-1}\ldots k_{-(N-3)} \\ k_1k_2k_3\ldots k_{N-1} & k_{-N}k_2k_3\ldots k_{N-1} & k_{-N}k_{-1}k_3\ldots k_{(N-1)} & \cdots & k_{-N}k_{-1}k_{-2}\ldots k_{-(N-2)} \end{pmatrix} \tag{6d}$$

For instance, for a cycle with four steps:

$$\Delta = k_1k_2k_3k_4 - k_{-1}k_{-2}k_{-3}k_{-4} \tag{7a}$$

$$\hat{M} = \begin{pmatrix} k_2k_3k_4 & k_{-1}k_3k_4 & k_{-1}k_{-2}k_4 & k_{-1}k_{-2}k_{-3} \\ k_3k_4k_1 & k_{-2}k_4k_1 & k_{-2}k_{-3}k_1 & k_{-2}k_{-3}k_{-4} \\ k_4k_1k_2 & k_{-3}k_1k_2 & k_{-3}k_{-4}k_2 & k_{-3}k_{-4}k_{-1} \\ k_1k_2k_3 & k_{-4}k_2k_3 & k_{-4}k_{-1}k_3 & k_{-4}k_{-1}k_{-2} \end{pmatrix} \tag{7b}$$

Conversion of Rate Constant to Energy Levels. While rate constants (k's) are the *lingua franca* of experimentalists, in QM calculations all states are described in terms of their relative energies in a reaction profile that is located during the computational procedure. A connection between energies and rate constants is given by the Eyring expression:

$$\begin{aligned} k'_i &= \frac{k_\mathrm{B}T}{h} e^{-\Delta G_i^{\ddagger}/k_\mathrm{b}T} = \frac{k_\mathrm{B}T}{h} e^{[G(I_{i-1})-G(T_i)]/k_\mathrm{b}T} \\ k'_{-i} &= \frac{k_\mathrm{B}T}{h} e^{-\Delta G_{-i}^{\ddagger}/k_\mathrm{b}T} = \frac{k_\mathrm{B}T}{h} e^{[G(I_i)-G(T_i)]/k_\mathrm{b}T} \end{aligned} \tag{8}$$

Here, $G(I_{i-1})$ is the free energy level of the intermediate preceding the transition state; the latter state energy is $G(T_i)$ (see Figure 2). For convenience, we can use the energies in $k_\mathrm{b}T$ units and employ the respective symbols I_i and T_i to denote dimensionless energies for the intermediates ($I_i = G(I_i)/k_\mathrm{b}T$) and the transition states ($T_i = G(T_i)/k_\mathrm{b}T$) at a specific temperature (for example, 1 kcal·mol^{-1}/RT = 1.7 dimensionless energy units at 298 K). In a similar fashion, we define the k's in $k_\mathrm{B}T/h$ units ($k_i = k'_i h/k_\mathrm{B}T$) to obtain the following expressions for the rate constants:

$$\begin{aligned} k_i &= e^{I_{i-1}-T_i} \\ k_{-i} &= e^{I_i-T_i} \end{aligned} \tag{9}$$

Degree of Rate Control ($X_{\mathrm{rc},i}$). The influence of a certain step on the rate of the reaction is a key question for any catalytic cycle. This influence can be quantified on the basis of Campbell's treatment, which defined the degree of rate control[14,15] as follows:

$$X_{\mathrm{rc},i} = \frac{k_i}{r}\frac{\partial r}{\partial k_i} = \frac{\partial \ln r}{\partial \ln k_i} \tag{10}$$

Here, $X_{\mathrm{rc},i}$ is the normalized variation of the global rate (r) of the cycle as a function of a change in an individual rate constant k_i; all other rate and equilibrium constants remain unaffected. A situation defined by $X_{\mathrm{rc},i} = 1$ would mean that the global reaction rate totally depends on step i, while $X_{\mathrm{rc},i} = 0$ would mean that a change of the rate constant of step i will not affect at all the observed kinetics of the cycle.

Using the symbols in eq 9. the degree of rate control becomes

$$X_{\mathrm{rc},i} = \left.\frac{\partial \ln r}{\partial \ln k_i}\right|_{K_m, k_{n\neq i,-i}} = -\frac{1}{r}\left.\frac{\partial r}{\partial T_i}\right|_{I_m, T_{n\neq i}} \tag{11}$$

where $X_{\mathrm{rc},i}$ is expressed in terms of the state energies (denoted as I_m and T_n).

Degree of TOF Control ($X_{\mathrm{TOF},i}$). On the basis of eq 11, we can define the *degree of TOF control* of a given state as follows:

$$X_{\mathrm{TOF},i} = \left|\frac{1}{\mathrm{TOF}}\frac{\partial \mathrm{TOF}}{\partial E_i}\right| \tag{12}$$

where E_i is a dimensionless energy of a transition state (T_i) or an intermediate (I_i). Since these two types of states influence the TOF in opposite directions, eq 12 uses an absolute magnitude sign, intended to unify the scale of TOF control values. The only states that are excluded from this equation are the reactants and products in the reaction profile, since their energies, as such, are not associated with the catalysis and the catalyst.

Calculation of $X_{\mathrm{TOF},i}$ for a Catalytic Cycle. From eq 12, and eq 6 for TOF, the degree of TOF control for a certain transition state i, with energy T_i, will be given by eq 13.

$$X_{\mathrm{TOF},T_i} = \left|\frac{1}{\mathrm{TOF}}\frac{\partial \mathrm{TOF}}{\partial T_i}\right| = \left|\frac{M}{\Delta}\left(\frac{\partial \Delta}{\partial T_i}\frac{1}{M} + \Delta\frac{\partial(1/M)}{\partial T_i}\right)\right| = \left|\frac{1}{\Delta}\frac{\partial \Delta}{\partial T_i} + M\frac{\partial(1/M)}{\partial T_i}\right| \tag{13}$$

To get an expression for the first term in eq 13, we can write Δ as a function of the state energies as follows:

$$\Delta = k_1k_2\cdots - k_{-1}k_{-2}\cdots = e^{I_0-T_1}e^{I_1-T_2}\cdots - e^{I_1-T_1}e^{I_2-T_2}\cdots \tag{14a}$$

$$\frac{\partial \Delta}{\partial T_i} = -e^{I_0-T_1}e^{I_1-T_2}\cdots + e^{I_1-T_1}e^{I_2-T_2}\cdots = -\Delta \tag{14b}$$

This leads to the following result for the first term in eq 13:

$$\frac{1}{\Delta}\frac{\partial \Delta}{\partial T_i} = -1 \tag{15}$$

For the second term in eq 13, we recall that M is the sum of the elements of the corresponding matrix $\hat{M}$ (see eq 6c). We may therefore write

$$M\frac{\partial(1/M)}{\partial T_i} = -\frac{1}{M}\sum_{ab}\frac{\partial M_{ab}}{\partial T_i} \tag{16}$$

where the M_{ab} terms are the elements of the matrix $\hat{M}$. Each of the derivatives under the summation symbol in eq 16 will be zero if the i state is not included, or $-M_{ab}$ if M_{ab} is a function of T_i. For instance, for a three-step cycle, the first element of the $\hat{M}$ matrix is

$$M_{11} = k_2k_3 = \mathrm{e}^{-T_2+I_1}\,\mathrm{e}^{-T_3+I_2} \tag{17a}$$

and therefore we have

$$\frac{\partial M_{11}}{\partial T_1} = 0$$
$$\frac{\partial M_{11}}{\partial T_2} = \frac{\partial M_{11}}{\partial T_3} = -M_{11} \tag{17b}$$

Let us label by M_{T_i} the sum of all elements that exclude T_i in the matrix $\hat{M}$; for example, for a two-step cycle we shall have

$$\hat{M} = \begin{pmatrix} k_2 & k_{-1} \\ k_1 & k_{-2} \end{pmatrix} = \begin{pmatrix} \mathrm{e}^{-T_2+I_1} & \mathrm{e}^{-T_1+I_1} \\ e^{-T_1+I_0} & \mathrm{e}^{-T_2+I_2} \end{pmatrix}$$
$$M_{T_1} = M_{1,1} + M_{2,2} = \mathrm{e}^{-T_2+I_1} + \mathrm{e}^{-T_2+I_2} \tag{17c}$$
$$M_{T_2} = M_{1,2} + M_{2,1} = \mathrm{e}^{-T_1+I_1} + \mathrm{e}^{-T_1+I_0}$$

Using this definition, we obtain the following general relation:

$$M\frac{\partial(1/M)}{\partial T_i} = -\frac{1}{M}\sum_{ab}\frac{\partial M_{ab}}{\partial T_i} = \frac{1}{M}(M - M_{T_i}) = 1 - \frac{M_{T_i}}{M} \tag{18}$$

These transformations lead to the final expression, shown in eq 19:

$$X_{\mathrm{TOF},T_i} = \left|\frac{1}{\Delta}\frac{\partial\Delta}{\partial T_i} + M\frac{\partial(1/M)}{\partial T_i}\right| = \frac{M_{T_i}}{M} \tag{19}$$

Since the sum of all M_{T_i} terms is equal to M (each element excludes from $\hat{M}$ only one T_i, in such a way that the sum of those terms that form M_{T_i} finally leads to the complete sum of all the elements), we get the following closure relationship for the TOF control quantities in the cycle:[17]

$$\sum_i X_{\mathrm{TOF},T_i} = \sum_i \frac{M_{T_i}}{M} = 1 \tag{20}$$

As a consequence of this relationship, *if the energy of the transition state in the rate-determining step of the cycle is lowered, the corresponding step will have a smaller X_{TOF,T_i} value, thus making all the other steps more relevant, acquiring larger TOF controls.*

The values of M_{T_i} can, in turn, be written as follows:

$$M_{T_i} = \mathrm{e}^{T_i}\,\mathrm{e}^{-\Sigma T_j}(\vec{G}_i\cdot\vec{P}_I) \tag{21a}$$

where T_j are the corresponding transition-state energies, $\vec{P}_I$ is a vector with elements

$$P_{I_i} = \mathrm{e}^{\Sigma I_i}\,\mathrm{e}^{-I_{(N-i+1)}} \tag{21b}$$

(N is the number of steps in the cycle), and $\vec{G}_i$ is a vector extracted from the ith row of the correction matrix $\hat{G}(\Delta G > 0)$:

$$\hat{G} = \begin{pmatrix} 1 & 1 & \dots & 1 \\ 1 & & 1 & e^{\Delta G} \\ \vdots & \iddots & \iddots & \vdots \\ 1 & e^{\Delta G} & \dots & e^{\Delta G} \end{pmatrix} \begin{matrix} \leftarrow \vec{G}_1 \\ \leftarrow \vec{G}_2 \\ \\ \leftarrow \vec{G}_N \end{matrix} \tag{21c}$$

This matrix shows that the transition states that are closer to the final stage (higher i index) have a higher X_{TOF,T_i} than would be expected solely from the energy level T_i. This is so because, for a transition state which is placed later in the sequence of the catalytic cycle, there corresponds a vector $\vec{G}_i$ with more coefficients $\mathrm{e}^{\Delta G}$ which act to upgrade the corresponding TOF control quantity.

M is calculated as the sum of the M_{T_i} (from eq 21),

$$M = \mathrm{e}^{-\Sigma T_i}[(\hat{G}\cdot\vec{P}_I)\cdot\vec{T}] \tag{22}$$

where $\vec{T}$ is a vector with elements $\exp(T_1)$, ..., $\exp(T_N)$. Now it can be shown that, when deriving X_{TOF,T_i} as a function of the state energies, we obtain the following quadratic form:

$$\frac{\partial X_{\mathrm{TOF},T_i}}{\partial T_i} = \frac{\partial\dfrac{M_{T_i}}{M}}{\partial T_i} = \frac{\partial\dfrac{\mathrm{e}^{T_i}(\vec{P}_I\cdot\vec{G}_i)}{\sum\mathrm{e}^{T_k}(\vec{P}_I\cdot\vec{G}_k)}}{\partial T_i}$$
$$= \frac{\mathrm{e}^{T_i}(\vec{P}_I\cdot\vec{G}_i)}{\sum\mathrm{e}^{T_k}(\vec{P}_I\cdot\vec{G}_k)} - \left(\frac{\mathrm{e}^{T_i}(\vec{P}_I\cdot\vec{G}_i)}{\sum\mathrm{e}^{T_k}(\vec{P}_I\cdot\vec{G}_k)}\right)^2 \tag{23}$$
$$\frac{\partial X_{\mathrm{TOF},T_i}}{\partial T_i} = X_{\mathrm{TOF},T_i} - {X_{\mathrm{TOF},T_i}}^2$$

$$\frac{\partial X_{\mathrm{TOF},T_j}}{\partial T_i} = \frac{\partial\dfrac{M_{T_j}}{M}}{\partial T_i} = \frac{\partial\dfrac{\mathrm{e}^{T_j}(\vec{P}_I\cdot\vec{G}_j)}{\sum\mathrm{e}^{T_k}(\vec{P}_I\cdot\vec{G}_k)}}{\partial T_i}$$
$$= -\frac{\mathrm{e}^{T_j}(\vec{P}_I\cdot\vec{G}_j)\,\mathrm{e}^{T_i}(\vec{P}_I\cdot\vec{G}_i)}{[\sum\mathrm{e}^{T_k}(\vec{P}_I\cdot\vec{G}_k)]^2} \tag{24}$$
$$\frac{\partial X_{\mathrm{TOF},T_j}}{\partial T_i} = -X_{\mathrm{TOF},T_j}X_{\mathrm{TOF},T_i}$$

As such, the influence (X_{TOF,T_i}, eq 23) of the transition state that undergoes stabilization will be lowered following an S-shaped curve (see Figure 5 later). At the same time, the other degrees of TOF control for transition states j (eq 24) will attain a mirror-image shape.

The calculation of the degree of TOF control of the intermediates ($X_{\mathrm{TOF},I_i} = M_{I_i}/M$) behaves in a symmetric fashion as follows:

$$M_{I_i} = \mathrm{e}^{-I_i}\,\mathrm{e}^{\sum_{j=1}^{N}I_j}(\vec{G'}_i\cdot\vec{P}_T) \tag{25a}$$

$$P_{T_i} = \mathrm{e}^{-\Sigma T_i}\,\mathrm{e}^{T_{(N-i+1)}} \tag{25b}$$

$$\hat{G'} = \begin{pmatrix} e^{\Delta G} & \dots & e^{\Delta G} & 1 \\ \vdots & \iddots & \iddots & \vdots \\ e^{\Delta G} & 1 & & 1 \\ 1 & \dots & 1 & 1 \end{pmatrix} \tag{25c}$$

Thus, the correction matrix $\hat{G}'$ scales the different steps in an inverse fashion to the matrix $\hat{G}$ in eq 21c, making the "early" intermediates (with smaller i index) more relevant than the others. In this notation, I_N is the product state and I_0 (that is not included explicitly in M_I) is

(17) This was presumed by Campbell.[14,15] Other examples of this relation for different systems can be found in the following: Corthright, R. D.; Dumesic, J. A. *Adv. Catal.* **2001**, *46*, 161−263. Barañski, A. *Solid State Ionics* **1999**, *117*, 123−128.

the reactant state. The same closure relation that links the degrees of TOF control for the various transition states applies to the sum of $\boldsymbol{X}_{\mathrm{TOF},I_i}$ quantities for the intermediates in the cycle, for which the sum is normalized to 1.

Calculation of TOF for a Catalytic Cycle—The Corrected Energetic Span. Having M (eq 22), we just need to derive Δ as follows:

$$\Delta = \mathrm{e}^{-\sum_{i=1}^{N} T_i}\, \mathrm{e}^{\sum_{i=1}^{N} I_i}(\mathrm{e}^{\Delta G} - 1) \tag{26}$$

$$\mathrm{TOF} = \frac{\Delta}{M} = \frac{\mathrm{e}^{\Delta G} - 1}{(\hat{G}\cdot\vec{I})\cdot\vec{T}} \tag{27}$$

where $\hat{G}$ is the correction matrix (eq 21c), $\vec{I}$ is the vector (exp($-I_N$), ..., exp($-I_1$)), and the vector $\vec{T}$ is (exp(T_1), ..., exp(T_N)). Equation 27, a direct consequence of Christiansen's treatment,[13] forms the basis for the algorithm used here to calculate efficiencies of catalytic cycles. From this expression we can see that the influence of the TOF of a given transition state increases as the transition state's energy increases and as it lies closer to the product phase in the sequence of the cycle. For the intermediates, the impact on the rate grows as their energy is lowered and as the intermediate is more proximal to the reactants.

Derivation of the Corrected Energetic Span. To have a quicker but still accurate estimate of the TOF and $X_{\mathrm{TOF},I}$, we can use *the corrected energetic span* ($\delta E'$). Mathematically, to calculate $\delta E'$ we have to neglect all terms but one in the denominator of the expression in eq 27 for the TOF calculation. This is usually a good approximation, considering that a difference of only 3 kcal/mol in two exponential terms creates a difference of 99% in their relative importance. In the numerator of eq 27, we may neglect the 1, since $\mathrm{e}^{\Delta G} \gg 1$. We finally obtain the following:[18]

$$\delta E' = \begin{cases} T_k - I_j & \text{if } k > j \\ T_k - I_j - \Delta G & \text{if } k \le j \end{cases} \qquad \Delta G > 0 \text{ (by defn)} \tag{28}$$

The above difference between the two expressions of the energetic span depends on the relative positions of the transition state and the intermediate.[18] For example, consider a two-step cycle characterized by the following matrices:

$$\hat{G} = \begin{pmatrix} 1 & 1 \\ 1 & \mathrm{e}^{\Delta G} \end{pmatrix} \tag{29a}$$

$$\vec{I} = (\mathrm{e}^{-I_2}, \mathrm{e}^{-I_1}) \tag{29b}$$

$$\vec{T} = (\mathrm{e}^{T_1}, \mathrm{e}^{T_2}) \tag{29c}$$

The TOF will be

$$\begin{aligned} \mathrm{TOF} &= \frac{\mathrm{e}^{\Delta G} - 1}{(\hat{G}\cdot\vec{I})\cdot\vec{T}} = \frac{\mathrm{e}^{\Delta G} - 1}{\mathrm{e}^{-I_2+T_1} + \mathrm{e}^{-I_1+T_1} + \mathrm{e}^{-I_2+T_2} + \mathrm{e}^{-I_1+T_2+\Delta G}} \\ &\approx \frac{\mathrm{e}^{\Delta G}}{\mathrm{e}^{-I_2+T_1} + \mathrm{e}^{-I_1+T_1} + \mathrm{e}^{-I_2+T_2} + \mathrm{e}^{-I_1+T_2+\Delta G}} \\ &= (\mathrm{e}^{-I_2+T_1-\Delta G} + \mathrm{e}^{-I_1+T_1-\Delta G} + \mathrm{e}^{-I_2+T_2-\Delta G} + \mathrm{e}^{-I_1+T_2})^{-1} \end{aligned} \tag{30}$$

Usually only the term with highest exponential value in eq 30, the one that maximizes δE, cannot be neglected. Therefore, we have eq 31, which approximates eq 30:

$$\mathrm{TOF} \approx \mathrm{e}^{-(-I_j+T_k\{-\Delta G\})} = \mathrm{e}^{-\delta E'} \tag{31}$$

In a case when two terms in eq 30 become relevant, for example with two transition states having high X_{TOF,T_i} (as it appears later in this paper for the Pd cross-coupling reaction), the resultant TOF will be

$$\begin{aligned} \mathrm{TOF} &\approx (\mathrm{e}^{-I_j+T_k\{-\Delta G\}} + \mathrm{e}^{-I_m+T_n\{-\Delta G\}})^{-1} \\ &= \frac{1}{1+\mathrm{e}^{-b}}\mathrm{e}^{-(-I_j+T_k\{-\Delta G\})} = \frac{1}{1+\mathrm{e}^{-b}}\mathrm{e}^{\delta E'} \end{aligned} \tag{32a}$$

where b is the difference of both exponential terms:

$$b = (I_j - T_k\{+\Delta G\}) - (I_m - T_n\{+\Delta G\}) \tag{32b}$$

and the energetic span is the bigger of the two terms. The factor $[1 + \exp(-b)]^{-1}$ is smaller than 1 and will lower the TOF of the cycle. For instance, if both exponential terms are equal (see an example in the Applications section later), then the TOF becomes simply $\exp(\delta E')/2$, and as such, the TOF of the cycle will be halved. Thus, for a given $\delta E'$, the TOF will be lowered with the increase of the number of combinations between intermediates and transition states having similar status in the cycle (eq 30).

From the definition in eq 12 and eq 32, we then find that, when two transition states have comparable importance in a cycle, the degree of TOF control will be

$$X_{\mathrm{TOF},T_i} = \frac{1}{1+\mathrm{e}^{-b}} \tag{33}$$

A Summary—How To Calculate the TOF. Once the full cycle is calculated by a QM method, one defines all the k_i's and equilibrium constant in energetic terms as defined above (eq 9). Strictly speaking, free energies are required. However, when these are not available (or are inaccurately determined by the QM method), one may cautiously use energies or energies with ZPE corrections to obtain some insight into the cycle. For accurate results, the TOF must be calculated from eq 27 and X_{TOF,T_i} from eq 19. However, in most cases (and in the cases studied later in this work) eq 27 can be rigorously replaced by the simpler expression in eq 34, when two combinations of intermediates and transition states are dominant, as appears on the exponential terms of eq 30. Alternatively, eq 31 may be applied for those cases where only one transition state and one intermediate are influential:

$$\mathrm{TOF} = \frac{1}{1+\mathrm{e}^{-b}}\mathrm{e}^{\delta E'} \tag{34a}$$

where

$$\delta E' = \begin{cases} T_k - I_j & \text{if } k > j \\ T_k - I_j - \Delta G & \text{if } k \le j \end{cases} \tag{34b}$$

Thus, as a rule of thumb, it is possible to reason about the TOF of a cycle by just measuring (calculating) the energy span between the MARI and the highest transition state if the latter appears in the cycle after the intermediate, or by subtracting from the same energy span the value of ΔG (ΔG defined always as a positive quantity) whenever the highest transition state appears before the intermediate (eq 34b, Figure 3).

QM Methods. The kinetic scheme is applied here to a few cycles computed previously by QM methods.

The cross-coupling reaction of an aryl halide with neutral and anionic Pd^0 catalyst was studied previously[2] using the B3LYP functional and the LACVP*+ basis set implemented in Jaguar 4.2.[19] All geometries were optimized with Jaguar 4.2, while the ZPE corrections were determined from Gaussian 98.[20] In the present study, we added to the various species free energy terms and single-point solvation energies. In the case of the cross-coupling of carboxylic anhydrides with

(18) The distinction in eq 28 is a consequence of the $\mathrm{e}^{\Delta G}$ terms in the correction matrix (and is also consistent with a change of the starting point to other intermediates).
(19) *Jaguar 4.2*; Schrödinger, Inc.: Portland, OR, 1991−2000.
(20) Frisch, M. J.; et al. *Gaussian 98*, Revision A.11.2; Gaussian, Inc.: Pittsburgh, PA, 2001.

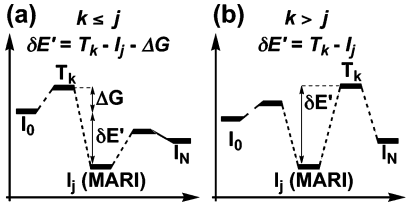

Figure 3. Corrected energetic span ($\delta E'$) for calculating TOF when the transition state with highest $X_{TOF,T}$ (T_k, the HETS) (a) comes before the intermediate with highest $X_{TOF,I}$ (I_j, the MARI) and (b) comes after this intermediate.

arylboronic acid,[3] the authors used the BP86 DFT functional with the 6-31G* basis set for all atoms except for Pd, which was described by the LANL2DZ basis set, implemented in Gaussian 98. The calculation of the Heck reaction with Ni and Pd[6] was carried out using B3LYP with the LANL2DZ//LANL2DZ(p) basis set (consisting of the LANL2DZ basis set with an extra d polarization function for P, Cl, Br, and I, an f function for Ni and Pd, and D95v(d) for H, C, and O).

Applications

Having established the connection between QM calculations and a basic kinetic model, we shall now use it to interrogate a few catalytic cycles that were computed by QM methods and published recently in the literature.[2,3,6] An additional application is to a longstanding effect in heterogeneous catalysis. The basic expressions that are needed for these applications are eqs 31−34. Already at the outset, we have to emphasize that reliable TOF values can be obtained *only from accurate calculations of free energies in a solvent*. However, accurate free energy calculations in a solvent are not commonly available, and therefore, in such cases, the efficiency of the computed cycle may be calculated using the energy scale employed in the calculations. Moreover, even when free energies are available, it is still instructive to obtain an analysis of the effects of the various energy components to the TOF, as is done in the first example below. As such, the following applications serve the purpose of projecting the insight of the model for the practicing computational chemist.

Cross-Coupling of an Aryl Halide with Neutral and Anionic Pd^0 Catalyst. The cross-coupling reaction[21] in eq 35 is catalyzed by divalent Pd^0 complexes. In a recent paper,[2] we

$$\mathrm{Ar{-}X + Nu^- \rightarrow Ar{-}Nu + X^-} \qquad (35)$$

studied two alternative catalytic cycles based on two different formulations of the catalyst. These two cycles are shown in Scheme 2; one involves the neutral PdL_2 (L = PR_3) catalyst, which appears in the consensus mechanism, and the other involves an anionic PdL_2X^- catalyst, proposed by Jutand and Amatore.[21] Experimentally, the R substituents of the phosphine are usually phenyl groups, X^- is a halide anion, and Nu^- is a boronic acid, a Grignard reagent, or a hard nuclephile.

The theoretical studies first established the existence of the anionic catalyst species for a variety of anions and phospine ligands (with PH_3, PPh_3, and PV_3; V = vinyl).[2,3,22,23] The anionic complex was shown to be a genuine minimum also in solution, using a continuum THF as solvent, and with a discrete cluster

Scheme 2. Neutral ("Consensus") and Anionic Mechanisms for Cross-Coupling[a]

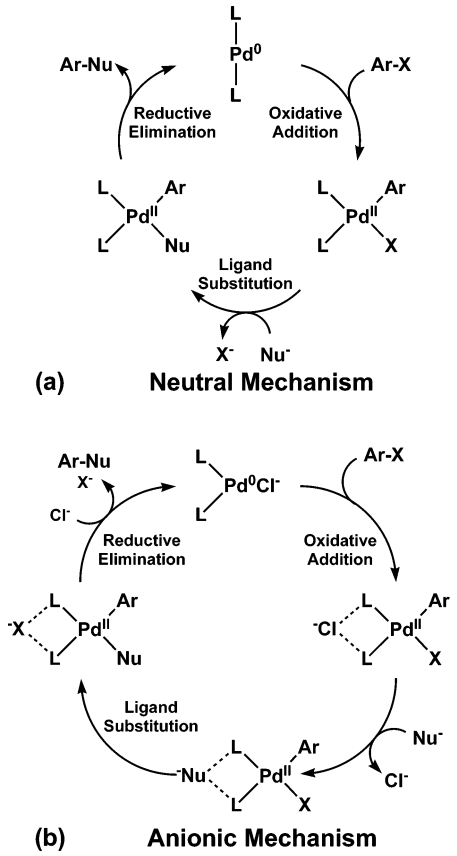

[a] The anionic mechanism follows ref 2.

of 7−10 THF molecules.[22] Similar tests that were carried out on other species in the cycle[24] showed that anionic additive remains as part of the structure also in a solvent. In addition, the role of the anionic catalyst for X^- = acetate, in the reaction with Ph−I, was discussed by Goossen et al.[3,23] for gas-phase and solution-phase conditions. The full catalytic cycles for the two mechanisms in Scheme 2[2] were computed using PH_3 as ligand models, Ph−Cl as reactant, and SH^- as nucleophile. These cycles were compared also with the characteristic cycles produced by neutral chelated catalysts $Pd(PH_2(CH_2)_nPH_2)$ (n = 3, 6).[2] It was argued that the anionic catalyst is superior to the neutral and bidentate catalysts, since the anionic additive lowers the energy of the HETS in the oxidative addition step and raises the energy of the MARI. However, this argument was based on *the uncorrected energy span* of the cycle (eq 3), which, as we argued above, may not always be an accurate measure of the TOF. Here, we apply the model discussed above.

The cycle energy profiles obtained in this study are represented in Figure 4, which is adapted from the original work in ref 2, where zero-point energy (ZPE) corrections were used. Table 1 collects the necessary data to apply the equations for

(21) (a) Amatore, C.; Jutand, A.; Medeiros, M. J.; Mottier, L. *J. Electroanal. Chem.* **1997**, *422*, 125−132. (b) Amatore, C.; Azzabi, M.; Jutand, A. *J. Am. Chem. Soc.* **1991**, *113*, 8375−8384. (c) Amatore, C.; Jutand, A.; Suarez, A. *J. Am. Chem. Soc.* **1993**, *115*, 9531−9541. (d) Amatore, C.; Jutand, A. *J. Organomet. Chem.* **1999**, *576*, 254−278. (d) Amatore, C.; Jutand, A. *Acc. Chem. Res.* **2000**, *33*, 314−321.

(22) Kozuch, S.; Shaik, S.; Jutand, A.; Amatore, C. *Chem. Eur. J.* **2004**, *10*, 3072−3080.

(23) Goossen, L. J.; Koley, D.; Hermann, H. L.; Thiel, W. *Organometallics* **2005**, *24*, 2398−2410.

(24) Similar tests for the HETS of the anionic cycle ($\mathbf{TS}_{H,Cl}^{Ox}$ in Figure 4) showed that the Cl^- anion remains nestled at the back of the phosphine ligand.[2] The survival of the MARI (in Figure 4) with a continuum THF model was also tested, and the MARI was found to be a genuine minimum, with some elongation of the average distance between the Cl^- and the phosphines (from 2.360 to 2.556 Å).

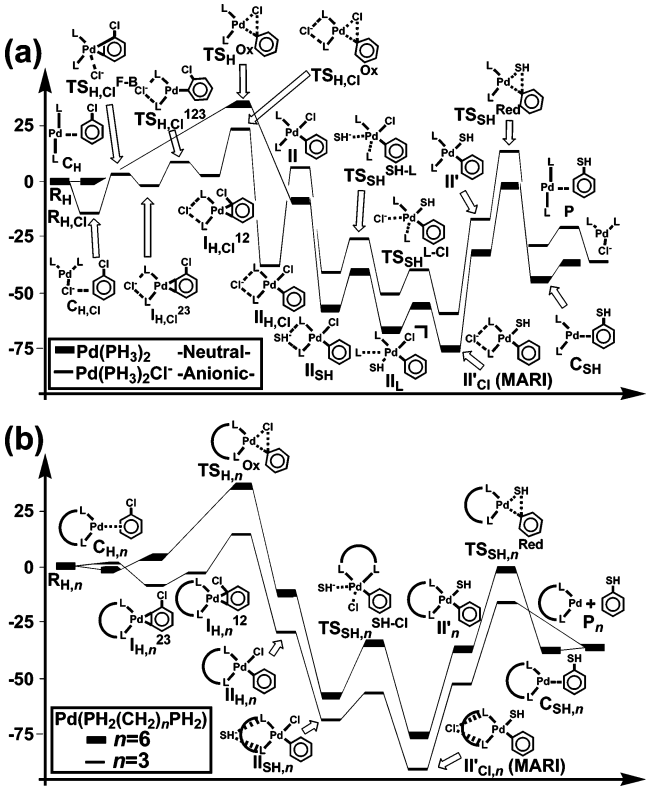

Figure 4. Full catalytic cycles for (a) anionic (PdL_2Cl^-) and neutral (PdL_2; L = PH_3) catalysts and (b) neutral catalysts with bidentate ligands (PH_2-$(CH_2)_nPH_2$) having six and three methylene links (energy values with ZPE corrections are given, dimensionless, at 298 K). Note that the reactants for the two cycles are placed together at zero energy, and consequently, the relative energies of other species are different in the two cycles even when the species are identical. A schematic anionic mechanism is shown in Scheme 2. Adapted from ref 2.

TOF and TOF control in the various putative cycles. The energies (corrected by ZPE) are expressed here in dimensionless units at 298 K. In the present treatment, we consider also the conclusions based on free energies and solvation corrections. Thus, this example may illustrate the capability of the model to discern alternative hypotheses and to pinpoint deficiencies in a given computed cycle.

Catalytic Cycle of the Neutral Catalyst with Monodentate Phosphine Ligands. The neutral mechanism (Figure 4a) involves concerted oxidative addition and reductive elimination. After oxidative addition of Ph−Cl, the intermediate **II** undergoes two consecutive steps of ligand substitution: the first involves displacement of the PH_3 ligand with the incoming nucleophile, HS^-, leading to $\mathbf{II}_L$, and subsequently, upon re-entering of the phosphine ligand, the Cl^- is displaced. The so-generated complex, $\mathbf{II'}_{Cl}$ in Figure 4a, is the MARI.[24] From a kinetic viewpoint, we take this "consensus" cycle as standard and assign it, in Table 1, a reference value of TOF = 1; the other cycles were estimated relative to this standard.

Using the data in Table 1, the resulting degree of TOF control for the MARI of the neutral cycle (species **II′** in Figure 4) is 1, as expected from the low energy of this intermediate species. As shown in Figure 5, artificial elevation of the energy value of this MARI will cause an exponential growth of the TOF up to the point where other intermediates in the cycle start to become relevant as TOF controllers. In parallel, as the MARI energy grows, the reaction rate reaches a plateau as a consequence of the decreased influence of this intermediate compared to the other ones. The $X_{TOF,i}$ profile for this stage is S-shaped like a titration profile, as described above in eqs 23 and 24.

Let us turn to consider the influence of the transition states in the cycle of the neutral catalyst in Figure 4a. Two states have considerable influence: the oxidative addition ($\mathbf{TS}_H^{Ox}$) and the reductive elimination ($\mathbf{TS}_{HS}^{Red}$), which have energetic spans that differ by $b = 0.6$ (from eq 33, $X_{TOF,T} = 0.65$ and 0.35, respectively). If it is chemically possible to lower only one of these two transition states, this will bring no great improvement of the cycle kinetics, as the unmodified step will eclipse the putative enhancement due to the lowering of the other transition state. Since the two steps have similar relationships to the MARI (see eq 32), the TOF approximation based on the corrected energetic span will be given by eq 36,

$$\mathrm{TOF} \approx \frac{1}{1+\mathrm{e}^{-b}}\,\mathrm{e}^{-(-I_{\mathrm{II'_{Cl}}}+T_{\mathrm{TS_H^{Ox}}}-\Delta G)} = 0.65\,\mathrm{e}^{-\delta E'} \quad (36)$$

where it is scaled by a factor of 0.65.

Catalytic Cycles of the Catalysts with Bidentate Phosphine Ligands. When the ligands of the catalysts are bidentate phosphines, R_2P-$(CH_2)_n$-PR_2, the smaller $(CH_2)_n$ linkers apply a uniform stabilization on the whole reaction profile energies in the catalytic cycle (see Figure 4b). For the linker with $n = 6$, the oxidative addition complex and the MARI have virtually the same energy levels as the corresponding species in the cycle of the neutral monodentate phospine-ligated complex (Figure 4a). It is therefore not surprising that the calculated relative TOF for $n = 6$ in Table 1 is 0.4. The degrees of TOF control have the same values as before; 1 for the MARI, and 0.71 and 0.29 for the oxidative addition and the reductive elimination, respectively. We note that the differences between TOF = 1 or 0.4 are not significant, *unless of course these were based on extremely accurate solvated free energy data*, which is usually not the case. Thus, the most one can say is that the cycles of the neutral $Pd^0(PR_3)_2$ and chelated $Pd^0[R_2P(CH_2)_nPR_2]$ catalysts have similar efficiencies, as calculated at the zero-point-corrected energy level in the gas phase.

The preceding conclusion is surprising in view of the usual conception that the bidentate-ligated Pd^0 complexes constitute superior catalysts, and the catalytic power improves with the decrease of the length of the $(CH_2)_n$ linker. Thus, the effect of the length of the linker on the oxidative addition has been studied before.[2,25] In both studies, it was found that the smaller the chain, the lower was the oxidative addition barrier, in line with predictions of the valence bond state correlation diagram model.[26] This conclusion, however, concerned only the rate-determining step of the cycle and did not take into account the energy of the MARI. Since the smaller the chain length is used, the more stable becomes the MARI, the two effects (barrier lowering and MARI stabilization) have opposite influences in the TOF, and therefore, the bidentate complexes have virtually identical TOFs, irrespective of the chain length (the relative TOF for the cycles of the chelated complex with $n = 3$ is 0.5 in Table 1).

In summary, the chelated catalysts do not improve the cycle kinetics. This is a consequence of the fact that the sum of the

(25) Su, M.; Chu, S. *Inorg. Chem.* **1998**, *37*, 3400−3406.
(26) (a) Shaik S.; Shurki A. *Angew. Chem., Int. Ed.* **1999**, *38*, 586−625; *Angew. Chem.* **1999**, *111*, 616−657. (b) Pross A.; Shaik S. *Acc. Chem. Res.* **1983**, *16*, 363. (c) Shaik, S.; Hiberty, P. C. *Rev. Comput. Quantum Chem.* **2004**, *20*, 1−100. (d) Shaik, S. S. *J. Am. Chem. Soc.* **1981**, *103*, 3692−3701.

Table 1. Key State Energies (corrected by ZPE, in dimensionless units) at 298 K, Degrees of TOF Control, Reaction Energies (ΔG), Energetic Span Values ($\delta E'$), and Relative TOF Values

		monodentate						neutral bidentate			
		neutral		anionic		anionic corrected		$n = 3$		$n = 6$	
$\Delta G = 36.5$[a]		E	X_{TOF}	E	X_{TOF}	E	X_{TOF}	E	X_{TOF}	E	X_{TOF}
intermediate	$\mathbf{II'}_{Cl}$	−74.9	1.00	−59.5	1.00	−59.5	1.00	−91.0	1.00	−75.6	1.00
transition states	$\mathbf{TS}_{H}^{Ox}$	34.9	0.65	22.9	0.00	22.9	0.55	13.7	0.00	35.3	0.71
	$\mathbf{TS}_{SH}^{Red}$	−2.2	0.35	13.2	1.00	−13.8	0.45	−16.6	1.00	−2.1	0.29
$\delta E'$		73.3		72.7		45.9		74.4		74.4	
relative TOF[b]		1		2.8		6.7×10^{11}		0.5		0.4	

[a] We use the generic symbol ΔG, as in the TOF equations, but actually this is a $\Delta(E + \text{ZPE})$ value. The quantity refers to the net process, $HS^- + Ph{-}Cl \rightarrow Ph{-}SH + Cl^-$. [b] These values are relative to the TOF of the neutral catalyst, $Pd(PH_3)_2$.

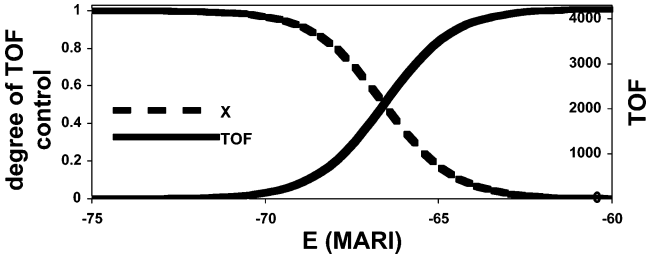

Figure 5. Evolution of the turnover frequency (TOF) and the degree of TOF control (X) of the neutral mechanism as a function of arbitrary destabilization of the MARI.

X_{TOF} for the intermediates is equal to the sum for the transition states, and therefore the two effects mutually cancel one another. Note that the TOF of the chelated catalysts is the same as that of the neutral $Pd^0(PR_3)_2$ complex, *despite the fact that the oxidative addition step of the latter has a barrier that is 12 kcal/mol higher than the former*. Only under conditions of a single turnover will the energy advantage of the barrier come into play, as indeed was found experimentally.[27]

Catalytic Cycles of Anionic Pd^0 Complexes in the Gas Phase. Previously,[2] it was argued that the anionic catalyst produces the main advantage of the chelate complexes without their drawback. As shown above in Figure 4a, when the reactant approaches the tricoordinated anionic catalyst, the Pd−Cl^- bond is broken. However, the departing Cl^- migrates to the site between the phosphine ligands ($\mathbf{I}_{H,Cl}$) and is clamped by Coulomb interactions with the positively charged hydrogen substituents of the ligands (the same was shown to be the case for PPh_3 ligands). This structural motif continues in the HETS, $\mathbf{TS}_{H,Cl}$, and was shown to survive in a solvent model.[2,24] Nestled in the phosphine cage, the chloride exerts on the phosphines a chainlike effect that produces a low-energy transition state for the oxidative addition step.[25,26] When the nucleophile approaches the catalyst, it displaces the chloride and assumes its position in the phosphine cage (species $\mathbf{II}_{H,Cl}$ to $\mathbf{II}_{SH}$ in Figure 4a). The loss of Coulomb stabilization of the Cl^- with the phosphines results in higher intermediates, relative to the onset of the cycle,than in the neutral cycle, where no anion is present before the nucleophile approaches.

For the catalytic cycle that appeared in the original paper (and is reproduced here in Figure 4a),[2] the anionic mechanism has a TOF of only 2.8 relative to the standard (see Table 1). This surprisingly small advantage was due to the fact that, in the treatment of the final stage of the catalytic cycle, we

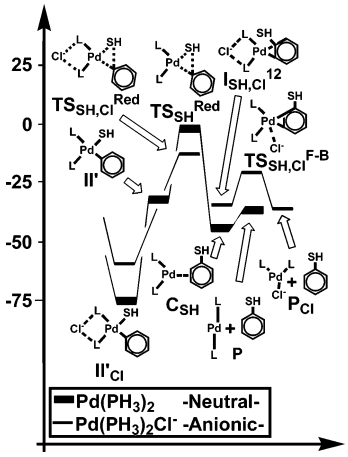

Figure 6. Revised energy profile plot (relative to Figure 4a) for the reductive elimination in the anionic and neutral cycles.

neglected the effect of the Cl^- anion (which was originally part of the Ph−Cl substrate). Originally,[2] without the kinetic model to guide us, we assumed that once this Cl^- anion departed there were no kinetically important steps. Only here, with the advent of the kinetic model, could we appreciate that this neglect leads to an underestimation of the influence of reductive elimination to the TOF and its degree of TOF control. Recalculation of this last step, as shown in Figure 6, reveals that the departing Cl^- ion is nestled again in the Coulomb cage near the phosphines, lowering the barrier for reductive elimination by the above-discussed chainlike effect.[2,25,26] This effect is precisely the same as the one exerted on the oxidative addition by the original Cl^- in the $Pd(PH_3)_2Cl^-$ catalyst. With this step taken into account, the resulting energetic spans taken from the oxidative addition and the reductive elimination become almost isoenergetic ($b = 0.2$ between these two transition states, resulting in TOF = 0.55 $\exp(\delta E)$). A calculation of $\delta E'$ in the corrected cycle gives us 45.9, and is therefore 27.4 energy units lower than the span of the cycle for the neutral catalyst (at 298 K, this is equivalent to 16.4 kcal/mol). The new TOF for the corrected anionic cycle, given in Table 1, is 6.7×10^{11} relative to the standard TOF = 1 for the neutral catalyst! This result seems to support the experimental data of Jutand and Amatore regarding the importance of the anionic catalyst for a working cycle.[10,21]

Comparison of the Catalytic Cycles of Neutral and Anionic Pd^0 Catalysts Using Free Energies and Solvation Corrections. The above discussion refers to gas-phase energies with ZPE corrections, and the question that remains is: how would the incorporation of free energies and solvation corrections affect this conclusion? The resulting parameters are shown in Table

(27) Portnoy, M.; Ben-Daviv, Y.; Rousso, I.; Milstein, D. *Organometallics* **1994**, *13*, 3465−3479.

Table 2. Energy Parameters (Dimensionless) at 298 K and TOFs for the Catalytic Cycles of the Neutral and Anionic Catalysts, Using Gas-Phase Energies with ZPE Correction, Gas-Phase Free Energies, and Gas-Phase Energies with ZPE and Polarizable Continuum Solvation Correction

		energy[a] $\Delta G^b = 36.5$		free energy $\Delta G^b = 35.9$		energy in solvent[a] $\Delta G^b = 41.3$	
		neutral	anionic	neutral	anionic	neutral	anionic
MARI	$\mathbf{II}'_{Cl}$	−74.9	−59.5	−40.5	−33.5	−43.4	−57.0
HETS	$\mathbf{TS}_{H}^{Ox}$	34.9	22.9	53.7	46.2	35.1	31.4
	$\mathbf{TS}_{SH}^{Red}$	−2.2	−13.8	19.6	12.7	−2.9	−7.5
$\delta E'$		73.3	45.9	60.2	46.2	40.6	49.5
relative TOF		1	6.7×10^{11}	1	1.2×10^{6}	1	1.2×10^{-4}

[a] Energy with ZPE correction. [b] The quantity refers to the net process, $HS^- + Ph{-}Cl \rightarrow Ph{-}SH + Cl^-$.

Scheme 3. Cross-Coupling of Carboxylic Anhydride with Arylboronic Acid, Studied in Ref 3

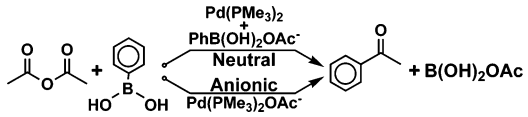

2. It is seen that, on the free energy scale, the anionic catalyst is still the better option, having a relative TOF of 1.2×10^6 compared with the neutral cycle. However, adding solvation energy correction (using a continuum THF model in Jaguar 4.2[19]) to the gas phase + ZPE correction inverts the order. Now the TOF of the cycle for the neutral catalyst is much higher than that of the anionic catalyst. The major effect is the relative change in the energy of the MARI that becomes deeper in energy with solvation, thereby raising the energy span of the anionic cycle; this is the case despite of the energy lowering of the HETS. This result is in discord with the experimental data of Jutand and Amatore regarding the importance of the anionic catalyst for a working cycle.[10,21]

In light of these new results, the final judgment on the role of anionic additive[10,21] will have to be based on more complex QM or QM/MM calculations of the cycle, *including the so far neglected counterion of the anionic additive*, and possibly with accurate free energy quantities. Nevertheless, this application demonstrates the importance of considering the entire cycle and not only selected states.

Cross-Coupling of Carboxylic Anhydrides with Arylboronic Acids. Goossen et al.[3] studied the cross-coupling reaction using two catalyst species, the neutral one, $Pd(PMe_3)_2$, and the anionic species, $Pd(PMe_3)_2OAc^-$, proposed by Jutand and Amatore,[10,21] with an arylboronic acid as nucleophile. The reaction mechanism was found to consist of three phases, oxidative addition, transmetalation, and reductive elimination, as in the preceding cycle. Scheme 3 shows briefly the two alternative catalysts. Thus, the transmetalation step made use of acetate for both catalyst species; for the anionic catalyst, the acetate was part of the catalyst complex itself, while for the neutral catalyst the acetate was part of the phenylboronic acid and acted as a cocatalyst.

Table 3 summarizes the critical parameters and TOFs of the two cycles. In both mechanisms, the states that maximize the energetic span are the same. The MARI is the starting point for the transmetalation (with free energy of −25.5 (dimensionless) for the anionic cycle, −8.4 for the neutral one at 298 K; in both cases this is relative to the reactant species). The most important transition state is the one involving the dissociation of the Ph−B bond. The resulting energetic span for the anionic

Table 3. Key Free Energies (in dimensionless units) at 298 K, Reaction Energy, Energetic Span, and the TOF Relative to the Neutral Mechanism

$\Delta G = 25.8$	neutral	anionic
intermediate	−8.4	−25.5
transition state	28.2	11.4
$\delta E'$	36.7	36.8
relative TOF	1	0.9

Scheme 4. Heck Reaction with Ni and Pd Complexes

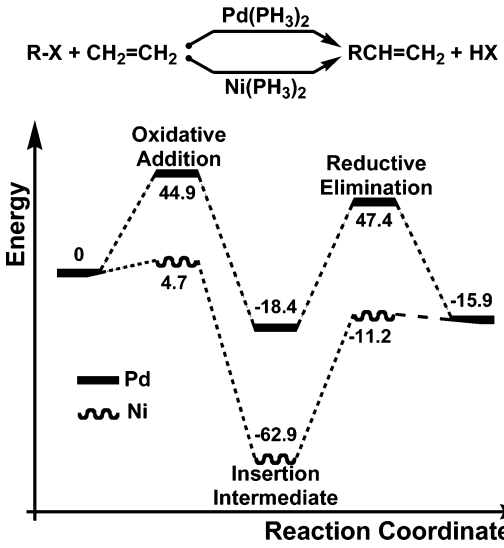

mechanism is 36.8, while for the neutral one it is 36.7 ($\delta E' = T - I$). Consequently, both catalytic cycles have virtually the same TOF.

Comparison of the Heck Reaction with Pd and Ni Catalysts. Theoretical calculations[6] of the Heck reaction catalyzed by two metal complexes of the divalent palladium(0) and nickel(0) species revealed the same mechanism for both catalysts. Since nickel is less electronegative than palladium, its oxidative addition step has a low-energy transition state leading to very stable intermediates. The oxidative addition is more difficult in the case of the palladium catalyst, and hence, the energy profile exhibits high transition states and intermediates. The two energy profiles are shown schematically in Scheme 4, along with indication of the critical states in the reaction.

At a superficial glance, we cannot favor one of the cycles in Scheme 4, and this is where the calculation of the corrected energetic span is handy. Again, for both catalysts the most influential intermediate is the insertion intermediate. For the Pd catalyst, the transition state for oxidative addition is the one

Table 4. Key Free Energies and Energetic Span (Dimensionless) for the Heck Reaction Catalyzed by Pd(0) and Ni(0) Complexes at 298 K

		Ni		Pd	
$\Delta G = 15.9$		E	X_{TOF}	E	X_{TOF}
intermediate	insertion	−62.9	1.0	−18.4	1.0
transition state	oxid addn	4.7	0.5	44.9	1.0
	red elimin	−11.2	0.5		
$\delta E'$		51.7		47.4	
relative TOF[a]		1		147	

[a] The TOF values are relative to the nickel mechanism as a standard.

Scheme 5. An Example of Sabatier's Volcano Curve for Formic Acid Decomposition as a Function of Different Metallic Catalysts[a]

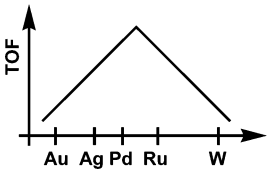

[a] From ref 5.

with the highest degree of TOF control. The corresponding data for TOF calculations are given in Table 4.

Using the data in Table 4, with due consideration of the ΔG quantity, the resulting energetic span for the Pd(0) catalyst is given by

$$\delta E'(\mathrm{Pd}) = T_{\text{ox add}} - I_{\text{insert.}} - \Delta G = 47.4 \qquad (37)$$

For the Ni(0) catalyst, the reductive elimination transition state is as important to the kinetics as the one for oxidative addition. Therefore, we have

$$\delta E'(\mathrm{Ni}) = T_{\text{ox add}} - I_{\text{insert.}} - \Delta G = T_{\text{red elim}} - I_{\text{insert.}} = 51.7 \qquad (38)$$

and the corresponding TOF is half the exponential of the energetic span because of the two influential transition states. Thus, the relative TOF of the two cycles is given then by eq 39:

$$\frac{\mathrm{TOF_{Pd}}}{\mathrm{TOF_{Ni}}} = \frac{e^{-\delta E_{\mathrm{Pd}}}}{0.5\, e^{-\delta E_{\mathrm{Ni}}}} = 147 \qquad (39)$$

We emphasize that this difference pertains to the energy data reported as such in the original literature and not to accurate free energies in a solvent. With this qualification in mind, we might say that the result in eq 39 favors the palladium catalyst over the nickel one.

Sabatier's Volcano Curve in Heterogeneous Catalysis. The volcano curve, first discovered by Sabatier for heterogeneous catalytic systems (for which he received the Nobel Prize in 1912), describes the shape of the TOF function when changing the transition metal catalyst surface across the periodic table. Thus, moving from left to right in the periodic table, it was noted that the change in the transition metal surface led to an increase of the TOF up to a maximum, after which the TOF decreased sharply, forming the volcano shape depicted in Scheme 5.[7,8] Another way of looking at Scheme 5 is that the volcano shape describes the variation of TOF as a function of the heat of formation of the intermediate compound.[5] This volcano shape of TOF is expected also for homogeneous systems when small changes are made in the catalyst, e.g., as the previously described adjustment of the bite angle of a chelate ligand[2,25] or small gradual decreases in ligand electronegativity, etc. In the discussion below, we show the simple physical mechanism behind the volcano shape of the TOF. In so doing, we identify also the features that maximize the TOF in a series of cycles. This is done using the kinetic model developed above and the well-known Brønsted−Bell−Evans−Polanyi (BEP) principle.[9]

Consider the BEP linear relation[7,9] for an elementary step,

$$E_a = \alpha\, \Delta E + \beta \qquad (40)$$

where ΔE is the reaction energy for this elementary step, E_a its activation energy, β a constant, and α a coefficient between 0 and 1. A generalized BEP relation that considers the transition-state and the intermediate energies in a cycle will give us the same linear relationship, which in our energy notations becomes the following:

$$T_i = \alpha I_j + \beta \qquad (41)$$

where i and j can be the states with highest $X_{\mathrm{TOF},i}$ (see Figure 7). In this case, a change in the intermediate will also alter the

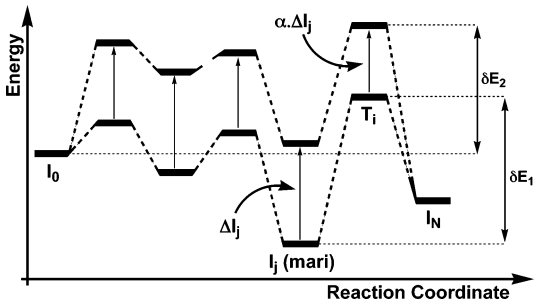

Figure 7. Elevation of the reaction profile by a change of a catalyst that maintains the mechanism of all elementary steps and responds to a BEP relation.

transition states, and the $X_{\mathrm{TOF},i}$ must display this effect. This is simply the celebrated Hammond postulate.[28]

For a catalyst that does not alter the nature of the elementary steps of the mechanism, what matter are energy changes in the energy profile. The two quantities that remain invariant for any catalyst in the series are the starting (I_0) and final (I_N) ones, shown in Figure 7. The reactant state, I_0, is always set to zero as a reference, while the product energy depends on the net reaction and is unaffected by the catalyst. If T_i and I_j are the states that determine the energetic span (lower profile in Figure 7),then we can write the following expression for the energy span:

$$\delta E_1 = T_i - I_j = (\alpha I_j + \beta) - I_j = I_j(\alpha - 1) + \beta \qquad (42)$$

The TOF of the cycle will then be

$$\mathrm{TOF_1} = e^{-\delta E_1} = e^{I_j(1-\alpha)-\beta} \qquad (43)$$

Since changes in the I_j state will induce changes in the other steps (except for states I_0 and I_N), we must consider the X_{TOF,I_j} based on the BEP relationship. So, fixing the states I_0 and I_N, we get

(28) Hammond, G. S. *J. Am. Chem. Soc.* **1955**, *77*, 334.

$$X_{\mathrm{TOF},I_j}|_{I_0,I_N} = \mathrm{e}^{-I_j(1-\alpha)+\beta}\,\frac{\partial \mathrm{e}^{I_j(1-\alpha)-\beta}}{\partial I_j} = 1-\alpha \qquad (44)$$

As such, a change of a catalyst that raises the intermediate energy (I_j) and obeys the BEP relation will change the TOF exponentially, giving rise to the left hillside of the volcano in Figure 8. If the energy of this MARI continues to grow, at a certain point the role of the MARI will pass on to the starting state I_0 (upper curve of Figure 7). At this point, the energetic span will be given by

$$\delta E_2 = T_i - I_0 \qquad (45a)$$

However, since T_i is still linked to I_j by the BEP relationship, we may re-express δE_2 as follows:

$$\delta E_2 = I_j\alpha + \beta - I_0 \qquad (45b)$$

Therefore, we obtain the following expression for TOF,

$$\mathrm{TOF}_2 = \mathrm{e}^{-\delta E_2} = \mathrm{e}^{-I_j\alpha-\beta+I_0} \qquad (46)$$

and for the TOF control,

$$X_{\mathrm{TOF},I_j}|_{I_0,I_N} = -\alpha \qquad (47)$$

As shown from eq 44 vs eq 47, the degree of TOF control changes sign when[29] $I_j = I_0$, and therefore the TOF will exhibit a maximum at this point (Figure 8) and a fall-down beyond it, as shown in Figure 8. This will result in a semblance to Sabatier's volcano shape. Having a maximum in the TOF function suggests that the best catalyst in a family of catalysts that share the same the elementary steps is the one leading to the lowest transition states while maintaining the initial state as the MARI of the cycle.

Conclusions

The kinetic model outlined here for catalytic cycles (based on Christiansen's treatment[13]) uses the energy quantities that are calculated in quantum chemical studies. A recent demonstration of the utility of coupling kinetic models to QM calculations is the treatment of polymerization by Michalak and Ziegler.[30] The model presented here allows a straightforward assessment of computed catalytic cycles and testing of alternative hypotheses. The efficiency of a catalytic cycle under steady-state conditions is determined by an energy span quantity, δE, which depends on the location of the highest energy transition state (HETS) and most stable intermediate (MARI) with respect to reactants and products. If the MARI precedes the HETS, δE is simply the energy difference between the two species in the cycle.[21] If the HETS appears before the MARI, the δE is corrected by subtracting the reaction energy ΔG. *The smaller the energetic span, the higher the turnover frequency of the cycle* (eq 34). The application of this simple idea to the catalytic cycles of the cross-coupling[2,3,21] and Heck[6] reactions and to Sabatier's volcano[7] shows that this model is useful for a critical assessment of the respective cycles and experimental findings. Further applications, which include free energies and proper solvation treatments, will be needed to appreciate its full potential and predictive ability.

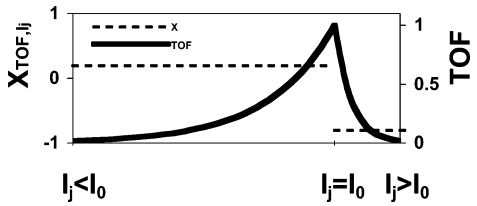

Figure 8. TOF and X_{TOF,I_j} for a BEP relation with $\alpha = 0.8$. The volcano shape appears as the lower energy intermediate goes from I_j to I_0.

Acknowledgment. This research was supported by the German Federal Ministry of Education and Research (BMBF) within the framework of the German−Israeli Project Cooperation (DIP).

Supporting Information Available: Full ref 20. This material is available free of charge via the Internet at http://pubs.acs.org.

JA0559146

(29) Note that the sign change is not apparent from eq 12, which uses absolute magnitudes for X_{TOF}.

(30) (a) Michalak, A.; Ziegler, T. *J. Am. Chem. Soc.* **2002**, *124*, 7519−7528. (b) Michalak, A.; Ziegler, T. *Organometallics* **2003**, *22*, 2069−2079.